

## Vibration suppression in ultrasonic machining described by non-linear differential equations<sup>†</sup>

M. M. Kamel, W. A. A. El-Ganaini and Y. S. Hamed<sup>\*</sup>

*Department of Engineering Mathematics, Faculty of Electronic Engineering, Menouf 32952, Egypt.*

(Manuscript Received February 28, 2008; Revised October 6, 2008; Accepted December 13, 2008)

---

### Abstract

Vibrations are usually undesired phenomena as they may cause damage or destruction of the system. However, sometimes they are desirable, as in ultrasonic machining (USM). In such case, the problem is a complicated one, as it is required to reduce the vibration of the machine head and have reasonable amplitude for the tool. In the present work, the coupling of two non-linear oscillators of the tool holder and tool representing ultrasonic cutting process is investigated. This leads to a two-degree-of-freedom system subjected to multi-external excitation force. The aim of this work is to control the tool holder behavior at simultaneous primary and internal resonance condition and have high amplitude for the tool. Multiple scale perturbation method is applied to obtain a solution up to the second order approximations. Other different resonance cases are reported and studied numerically. The stability of the system is investigated applying both phase-plane and frequency response techniques. The effects of the different parameters of the tool on the system behavior are studied numerically. Comparison with the available published work is reported.

*Keywords:* Vibration control; Stability; Ultrasonic machining (USM)

---

### 1. Introduction

Mechanical and structural systems are inherently non-linear due to many sources. Non-linearities necessarily introduce a whole range of phenomena that are not found in linear systems [1], including jump phenomena, occurrence of multiple solutions, modulations, shift in natural frequencies, the generation of combination resonances and chaotic motions [2–4]. In such systems, vibrations are needed to be controlled to minimize or eliminate the hazard of damage or destruction. There are two main regimes for vibration control: passive and active control. One of the most effective tools of passive vibration control is the dynamic absorber or the damper or the neutralizer [5]. Asfar, Eissa and El-Bassiouny [6–8] investigated the effects of a non-linear elastomeric torsional absorber

to control the vibrations of the crankshaft in internal combustion engines, when subject to external excitation torque. They reported that absorbers are very effective in reducing the vibrations of mechanical systems or structures. Lee et al. [9] demonstrated a dynamic vibration absorber system, which can be used to reduce speed fluctuations in a rotating machinery. Eissa [10] has shown that to control the vibration of a system subjected to harmonic excitations, the fundamental or the first harmonic absorber is the most effective one. Eissa and El-Ganaini [11, 12] studied the control of both vibration and dynamic chaos of a mechanical system having quadratic and cubic non-linearities, subjected to harmonic excitation using multi-absorbers. Eissa et al. [13–15] investigated saturation phenomena in non-linear oscillating systems subject to multi-parametric and/or external excitations. The system represents the vibration of a single-degree-of-freedom cantilever or the wing of an aircraft. They reported the occurrence of saturation phenomena at different parameter values. They ap-

<sup>†</sup> This paper was recommended for publication in revised form by Associate Editor Eung-Soo Shin

<sup>\*</sup> Corresponding author. Tel.: +2020103942917, Fax.: +20483660716  
E-mail address: eng\_yaser\_salah@yahoo.com

© KSME & Springer 2009

plied saturation values of different parameters as optimum working conditions for vibration suppression of the cantilever. Eissa et al. [16, 17] presented tuned absorbers in both transverse and longitudinal directions of a simple pendulum which was designed to control one frequency at primary resonance. They demonstrated the effectiveness of the absorber for passive control. They reported that the vibration of the system can be controlled actively via negative velocity feedback. Eissa et al. [18-20] studied both passive and active vibration control in some non-linear differential equations describing the vibration of an aircraft wing subject to multi-excitation forces, multi-parametric excitations with 1:2, 1:4 and 1:2:4 internal resonance active controllers, and demonstrated the effectiveness of such controllers. Lim et al. [21] studied the behavior of the (USM) hypothesized theoretical model. The theoretical results showed that controlled variations in the softening stiffness can have a significant effect on the overall non-linear response of the system, by making the overall effect hardening, softening, or approximately linear. Experimentally, it has also been demonstrated that coupling of ultrasonic components with different non-linear characteristics can strongly influence the performance of the system. Amer [22] investigated the coupling of two non-linear oscillators of the main system and absorber representing ultrasonic cutting process subjected to parametric excitation forces. A threshold value of main system linear damping has been obtained, where vibration can be reduced dramatically. This threshold value can be used effectively for passive vibration control, if it is economical. This will be more useful than usual passive control. It is simple and can be applicable for all excitation frequencies.

The objective of this work is to study a model subject to multi-external excitation forces. The model is represented by a two-degree-of-freedom system consisting of the tool holder and tool simulating the ultrasonic machining process. The multiple time scale perturbation technique is applied throughout to get an approximate solution up to the second order approximation. The stability of the system is investigated numerically by applying both phase-plane and frequency response function. The effects of the different parameters of the tool on system behavior are studied numerically. Comparison with the available published work is reported.

## 2. Mathematical modeling

Fig. 1 presents the actual ultrasonic machining and its simulation by a two-degree-of-freedom system consisting of the tool holder (machine head) and tool. The tool holder is excited by multi-external forces as shown in the following equations:

$$m_1 \ddot{X}_1 + \varepsilon c_1 \dot{X}_1 + \varepsilon c_2 (\dot{X}_1 - \dot{X}_2) + \varepsilon^2 c_3 \dot{X}_1^2 + k_1 X_1 + \varepsilon k_2 (X_1 - X_2) + \varepsilon h_1 X_1^3 + \varepsilon h_2 (X_1 - X_2)^2 - \varepsilon h_3 (X_1 - X_2)^3 + \varepsilon^2 h_4 X_1^5 = \varepsilon \sum_{j=1}^n f_j \cos j\Omega t \quad (a)$$

$$m_2 \ddot{X}_2 + \varepsilon c_2 (\dot{X}_2 - \dot{X}_1) + k_2 (X_2 - X_1) + \varepsilon h_2 (X_2 - X_1)^2 - \varepsilon h_3 (X_2 - X_1)^3 = 0 \quad (b)$$

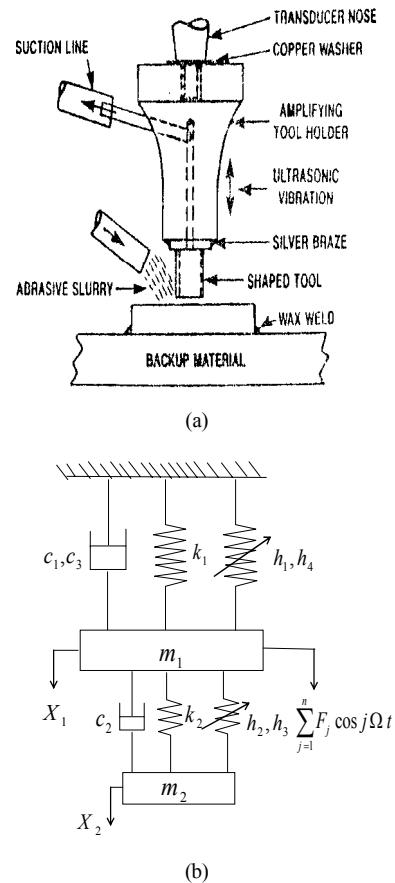


Fig. 1. (a) Ultrasonic machine (USM), (b) Schematic diagram of USM.

Dividing Eq. (a) by  $m_1$  and Eq. (b) by  $m_2$ , we obtain:

$$\begin{aligned} \ddot{X}_1 + 2\varepsilon\zeta_1\dot{X}_1 + 2\varepsilon\zeta_2(\dot{X}_1 - \dot{X}_2) + \varepsilon^2\zeta_3\dot{X}_1^2 \\ + \omega_1^2 X_1 + \varepsilon\gamma_1(X_1 - X_2) + \varepsilon\eta_1 X_1^3 + \varepsilon\eta_2(X_1 - X_2)^2 \\ - \varepsilon\eta_3(X_1 - X_2)^3 + \varepsilon^2\eta_4 X_1^5 = \varepsilon \sum_{j=1}^n F_j \cos j\Omega t \end{aligned} \quad (1)$$

$$\begin{aligned} \ddot{X}_2 + 2\varepsilon\zeta_4(\dot{X}_2 - \dot{X}_1) + \omega_2^2(X_2 - X_1) \\ + \varepsilon\eta_5(X_2 - X_1)^2 - \varepsilon\eta_6(X_2 - X_1)^3 = 0 \end{aligned} \quad (2)$$

where all parameters of Eqs. (1)-(2) are defined in the nomenclature. Non-linear terms are practically present in the stiffness and damping of all materials. Usually, even power non-linear terms are not present in stability analysis. We demonstrate that we included it just once in tool equations.

**2.1 Perturbation analysis**

Multiple scale perturbation method is conducted to obtain an approximate solution for Eqs. (1) and (2). Assume the solution in the form,

$$X_1(t; \varepsilon) = x_{10}(T_0, T_1) + \varepsilon x_{11}(T_0, T_1) + O(\varepsilon^2) \quad (3)$$

$$X_2(t; \varepsilon) = x_{20}(T_0, T_1) + \varepsilon x_{21}(T_0, T_1) + O(\varepsilon^2) \quad (4)$$

and the time derivatives become

$$\frac{d}{dt} = D_0 + \varepsilon D_1, \quad \frac{d^2}{dt^2} = D_0^2 + 2\varepsilon D_0 D_1 \quad (5)$$

where  $T_n = \varepsilon^n t$ . ( $n=0, 1$ ) are the fast and slow time scales, respectively.

Substituting Eqs. (3), (4) and (5) into Eqs. (1) and (2), and equating the coefficients of the same power of  $\varepsilon$  in both sides, we obtain

$$(D_0^2 + \omega_1^2)x_{10} = 0 \quad (6)$$

$$(D_0^2 + \omega_2^2)x_{20} = \omega_2^2 x_{10} \quad (7)$$

$$\begin{aligned} (D_0^2 + \omega_1^2)x_{11} = \sum_{j=1}^n F_j \cos j\Omega T_0 - 2(D_1 + \zeta_1 + \zeta_2) \\ \times (D_0 x_{10}) + 2\zeta_2 D_0 x_{20} - \gamma_1(x_{10} - x_{20}) \\ - \eta_1 x_{10}^3 - \eta_2(x_{10} - x_{20})^2 + \eta_3(x_{10} - x_{20})^3 \end{aligned} \quad (8)$$

$$\begin{aligned} (D_0^2 + \omega_2^2)x_{21} = -2D_0 D_1 x_{20} + 2\zeta_4 D_0 x_{10} \\ - 2\zeta_4 D_0 x_{20} + \omega_2^2 x_{11} - \eta_5(x_{10} - x_{20})^2 - \eta_6(x_{10} - x_{20})^3 \end{aligned} \quad (9)$$

The solution of Eq. (6) can be expressed in the form

$$x_{10} = A_1 \exp(i\omega_1 T_0) + cc \quad (10)$$

Using Eq. (10) into Eq. (7) yields

$$x_{20} = B_1 \exp(i\omega_2 T_0) + \Gamma A_1 \exp(i\omega_1 T_0) + cc \quad (11)$$

Where  $\Gamma = \frac{\omega_2^2}{\omega_2^2 - \omega_1^2}$  and  $A_1, B_1$  are complex functions in  $T_1$ , which can be determined from eliminating the secular terms at the next approximation, and cc, stands for the conjugate of the preceding terms. Substituting Eqs. (10) and (11) into Eq. (8), eliminating the secular terms, then the first order approximation is given by:

$$\begin{aligned} x_{11} = \sum_{j=1}^n E_j \exp(ji\Omega T_0) + E_2 \exp(i\omega_2 T_0) \\ + E_3 \exp(2i\omega_1 T_0) + E_4 \exp(2i\omega_2 T_0) \\ + E_5 \exp(3i\omega_1 T_0) + E_6 \exp(3i\omega_2 T_0) \\ + E_7 \exp(i(\omega_1 + \omega_2)T_0) + E_8 \exp(i(\omega_1 - \omega_2)T_0) \\ + E_9 \exp(i(\omega_1 + 2\omega_2)T_0) + E_{10} \exp(i(\omega_1 - 2\omega_2)T_0) \\ + E_{11} \exp(i(2\omega_1 + \omega_2)T_0) \\ + E_{12} \exp(i(2\omega_1 - \omega_2)T_0) + E_{13} + cc \end{aligned} \quad (12)$$

where  $E_s$  ( $s=1,2,\dots,13$ ) are complex functions in  $T_1$  and  $j=(1\dots n)$ ; for simplicity we take  $n=2$  in the study of stability. From Eqs. (10), (11) and (12) into Eq. (9) and eliminating the secular terms, the solution is given by:

$$\begin{aligned} x_{21} = \sum_{j=1}^n H_j \exp(ji\Omega T_0) + H_8 \exp(i\omega_1 T_0) \\ + H_3 \exp(2i\omega_1 T_0) + H_4 \exp(2i\omega_2 T_0) \\ + H_5 \exp(3i\omega_1 T_0) + H_6 \exp(3i\omega_2 T_0) \\ + H_7 \exp(i(\omega_1 + \omega_2)T_0) + H_8 \exp(i(\omega_1 - \omega_2)T_0) \\ + H_9 \exp(i(\omega_1 + 2\omega_2)T_0) + H_{10} \exp(i(\omega_1 - 2\omega_2)T_0) \\ + H_{11} \exp(i(2\omega_1 + \omega_2)T_0) + H_{12} \exp(i(2\omega_1 - \omega_2)T_0) \\ + H_{13} + cc \end{aligned} \quad (13)$$

where  $H_s$  ( $s=1,2,\dots,13$ ) are complex functions in  $T_1$  and  $j=(1\dots n)$ . The reported resonance cases at this approximation order are:

- (a) Trivial resonance:  $\Omega \cong \omega_1 \cong \omega_2 = 0$
- (b) Primary resonance:  $\Omega \cong \omega_1, \Omega \cong \omega_2$
- (c) Sub-harmonic resonance:  $\Omega \cong 2\omega_1, \Omega \cong 3\omega_1, \Omega \cong 2\omega_2, \Omega \cong 3\omega_2$
- (d) Super-harmonic resonance:  $\Omega \cong \omega_1/2, \Omega \cong \omega_1/3, \Omega \cong \omega_2/2, \Omega \cong \omega_2/3$

(e) Internal resonance:

$$\begin{aligned} \omega_1 &\cong 2\omega_2, \omega_1 \cong 3\omega_2, \omega_1 \cong 4\omega_2, \omega_1 \cong 5\omega_2, \\ \omega_2 &\cong 2\omega_1, \omega_2 \cong 3\omega_1, \omega_2 \cong 4\omega_1, \omega_2 \cong 5\omega_1, \\ 2\omega_1 &\cong 3\omega_2, 2\omega_1 \cong 5\omega_2, 3\omega_1 \cong 2\omega_2, 3\omega_1 \cong 5\omega_2, \\ 5\omega_1 &\cong 2\omega_2, 5\omega_1 \cong 3\omega_2 \end{aligned}$$

(f) Combined resonance:

$$\Omega \cong (\omega_1 + \omega_2), \Omega \cong \pm(\omega_1 - \omega_2)$$

Simultaneous or incident resonance: Any combination of the above resonance cases is considered as simultaneous resonance.

### 2.2 Stability of the system

Here, we investigate the stability at simultaneous primary and internal resonance cases. We introduce the detuning parameters  $\sigma_1$  and  $\sigma_2$  such that,

$$\Omega \cong \omega_1 + \varepsilon\sigma_1, \omega_2 \cong \omega_1 + \varepsilon\sigma_2 \tag{14}$$

This case represents the system worst case and at the same time tool or tool high amplitude. Substituting Eq. (14) into Eqs. (8) and (9) and eliminating the secular terms, leads to the solvability conditions for the first order approximation, and noting that  $A_1$  and  $B_1$  are functions in  $T_1$  we get

$$\begin{aligned} 2i\omega_1[D_1A_1 + \zeta_1A_1 + \zeta_2A_1] + \gamma_1A_1 + 3\eta_1A_1^2\bar{A}_1 \\ - 3\eta_3A_1^2\bar{A}_1 - 6\eta_3A_1B_1\bar{B}_1 - \frac{F_1}{2}e^{i\sigma_1T_1} - [2i\omega_2B_1\zeta_2 \\ + \gamma_1B_1 - 3\eta_3B_1^2\bar{B}_1 - 6\eta_3A_1\bar{A}_1B_1]e^{i\sigma_2T_1} \\ - [3\eta_3\bar{A}_1B_1^2]e^{2i\sigma_2T_1} + [3\eta_3A_1^2\bar{B}_1]e^{-i\sigma_2T_1} = 0 \end{aligned} \tag{15}$$

$$\begin{aligned} 2i\omega_2[D_1B_1 + \zeta_4B_1] - 3\eta_6B_1^2\bar{B}_1 - 6\eta_6A_1\bar{A}_1B_1 \\ + [3\eta_6\bar{A}_1B_1^2]e^{i\sigma_2T_1} - [2i\omega_1\zeta_4A_1 - 3\eta_6A_1^2\bar{A}_1 \\ - 6\eta_6A_1B_1\bar{B}_1]e^{-i\sigma_2T_1} - [3\eta_6A_1^2\bar{B}_1]e^{-2i\sigma_2T_1} = 0 \end{aligned} \tag{16}$$

Putting  $A_1 = \frac{1}{2}a_1(T_1)e^{i\psi_1(T_1)}$ ,  $B_1 = \frac{1}{2}b_1(T_1)e^{i\phi_1(T_1)}$  (17)

where  $a_1, b_1$  and  $\psi_1, \phi_1$  are the steady state amplitudes and the phases of the motion, respectively. Substituting Eq. (17) into Eqs. (15) and (16) and separating real and imaginary part yields,

$$a_1' = -(\zeta_1 + \zeta_2)a_1 + \frac{\omega_2\zeta_2b_1}{\omega_1}\cos\theta_2 + \left[ \frac{\gamma_1b_1}{2\omega_1} - \right.$$

$$\left. \frac{3\eta_3b_1^3}{8\omega_1} - \frac{3\eta_3a_1^2b_1}{8\omega_1} \right] \sin\theta_2 + \frac{F_1}{2\omega_1}\sin\theta_1 + \frac{3\eta_3a_1b_1^2}{8\omega_1}\sin 2\theta_2 \tag{18}$$

$$\begin{aligned} a_1\psi_1' &= \frac{\gamma_1a_1}{2\omega_1} - \frac{3(\eta_3 - \eta_1)a_1^3}{8\omega_1} - \frac{3\eta_3a_1b_1^2}{4\omega_1} - \left[ \frac{\gamma_1b_1}{2\omega_1} - \right. \\ &\left. \frac{3\eta_3b_1^3}{8\omega_1} - \frac{9\eta_3a_1^2b_1}{8\omega_1} \right] \cos\theta_2 + \frac{\omega_2\zeta_2b_1}{\omega_1}\sin\theta_2 - \frac{F_1}{2\omega_1}\cos\theta_1 \\ &- \frac{3\eta_3a_1b_1^2}{8\omega_1}\cos 2\theta_2 \end{aligned} \tag{19}$$

$$\begin{aligned} b_1' &= -\zeta_4b_1 + \frac{\omega_1\zeta_4a_1}{\omega_2}\cos\theta_2 + \left[ \frac{3\eta_6a_1^3}{8\omega_2} + \frac{3\eta_6a_1b_1^2}{8\omega_1} \right] \sin\theta_2 \\ &+ \frac{3\eta_3a_1^2b_1}{8\omega_1}\sin 2\theta_2 \end{aligned} \tag{20}$$

$$\begin{aligned} b_1\phi_1' &= -\frac{3\eta_6b_1^3}{8\omega_2} - \frac{3\eta_6a_1^2b_1}{4\omega_2} + \left[ \frac{3\eta_6a_1^3}{8\omega_2} + \frac{9\eta_6a_1b_1^2}{8\omega_1} \right] \cos\theta_2 \\ &- \frac{\omega_1\zeta_4a_1}{\omega_2}\sin\theta_2 - \frac{3\eta_3a_1^2b_1}{8\omega_2}\cos 2\theta_2 = 0 \end{aligned} \tag{21}$$

where

$$\theta_1 = \sigma_1T_1 - \psi_1, \theta_2 = \sigma_2T_1 + \phi_1 - \psi_1 \tag{22}$$

For steady state solutions,  $a_1' = b_1' = \theta_1' = \theta_2' = 0$ . Then from Eq. (22), we get:

$$\psi_1' = \sigma_1, \phi_1' = \sigma_1 - \sigma_2 \tag{23}$$

It follows from Eqs. (18)-(21) that the steady state solutions are given by

$$\begin{aligned} -(\zeta_1 + \zeta_2)a_1 + \frac{\omega_2\zeta_2b_1}{\omega_1}\cos\theta_2 + \left[ \frac{\gamma_1b_1}{2\omega_1} - \frac{3\eta_3b_1^3}{8\omega_1} \right. \\ \left. - \frac{3\eta_3a_1^2b_1}{8\omega_1} \right] \sin\theta_2 + \frac{F_1}{2\omega_1}\sin\theta_1 + \frac{3\eta_3a_1b_1^2}{8\omega_1}\sin 2\theta_2 = 0 \end{aligned} \tag{24}$$

$$\begin{aligned} a_1\sigma_1 &= \frac{\gamma_1a_1}{2\omega_1} - \frac{3(\eta_3 - \eta_1)a_1^3}{8\omega_1} - \frac{3\eta_3a_1b_1^2}{4\omega_1} - \left[ \frac{\gamma_1b_1}{2\omega_1} - \right. \\ &\left. \frac{3\eta_3b_1^3}{8\omega_1} - \frac{9\eta_3a_1^2b_1}{8\omega_1} \right] \cos\theta_2 + \frac{\omega_2\zeta_2b_1}{\omega_1}\sin\theta_2 - \frac{F_1}{2\omega_1}\cos\theta_1 \\ &- \frac{3\eta_3a_1b_1^2}{8\omega_1}\cos 2\theta_2 \end{aligned} \tag{25}$$

$$\begin{aligned} -\zeta_4b_1 + \frac{\omega_1\zeta_4a_1}{\omega_2}\cos\theta_2 + \left[ \frac{3\eta_6a_1^3}{8\omega_2} + \frac{3\eta_6a_1b_1^2}{8\omega_1} \right] \sin\theta_2 \\ + \frac{3\eta_3a_1^2b_1}{8\omega_1}\sin 2\theta_2 = 0 \end{aligned} \tag{26}$$

Table 1. Frequency response equations.

No	Cases	Frequency response equations (FRE)
1	$a_1 \neq 0, b_1 = 0$	$\sigma_1^2 + k_1\sigma_1 + k_2 = 0$
2	$a_1 = 0, b_1 \neq 0$	$\sigma_2^2 + k_3\sigma_2 + k_4 = 0$
3	$a_1 \neq 0, b_1 \neq 0$	$\sigma_1^2 + k_5\sigma_1 + k_6 = 0$ and $\sigma_2^2 + k_7\sigma_2 + k_8 = 0$

$$b_1(\sigma_1 - \sigma_2) = -\frac{3\eta_6 b_1^3}{8\omega_2} - \frac{3\eta_6 a_1^2 b_1}{4\omega_2} + \left[ \frac{3\eta_6 a_1^3}{8\omega_2} + \frac{9\eta_6 a_1 b_1^2}{8\omega_1} \right] \cos \theta_2 - \frac{\omega_1 \zeta_4 a_1}{\omega_2} \sin \theta_2 - \frac{3\eta_3 a_1^2 b_1}{8\omega_2} \cos 2\theta_2 = 0 \tag{27}$$

From Eqs. (24)-(27) we have the following cases:

- (1)  $a_1 \neq 0, b_1 = 0$  (Tool is ineffective)
- (2)  $a_1 = 0, b_1 \neq 0$  (Ideal case)
- (3)  $a_1 \neq 0, b_1 \neq 0$  (Practical case)

Table (1) gives the results of the frequency response equations.

Where  $k_1, k_2, k_3, k_4, k_5, k_6, k_7$  and  $k_8$  are defined in the appendix.

The stability of the linear solution of the obtained fixed points will be determined as follows. Consider  $A_1, B_1$  in the form:

$$A_1 = \frac{1}{2}[p_1 - iq_1]e^{iv_1 T_1}, \quad B_1 = \frac{1}{2}[p_2 - iq_2]e^{iv_2 T_1} \tag{28}$$

where  $p_1, p_2, q_1$  and  $q_2$  are real and  $v_1 = \sigma_1, v_2 = (\sigma_1 - \sigma_2)$ . Substituting Eq. (28) into the linear part of Eqs. (15) and (16) and separating real and imaginary part yields,

$$p_1' + (\zeta_1 + \zeta_2)p_1 + \left( v_1 - \frac{\gamma_1}{2\omega_1} \right) q_1 - \frac{\omega_2 \zeta_2}{\omega_1} p_2 + \frac{\gamma_1}{2\omega_1} q_2 = 0 \tag{29}$$

$$q_1' + (\zeta_1 + \zeta_2)q_1 - \left( v_1 - \frac{\gamma_1}{2\omega_1} + \frac{F_1}{2\omega_1 p_1} \right) p_1 - \frac{\omega_2 \zeta_2}{\omega_1} q_2 - \frac{\gamma_1}{2\omega_1} p_2 = 0 \tag{30}$$

$$p_2' + \zeta_4 p_2 - v_2 q_2 - \frac{\omega_1 \zeta_4}{\omega_2} p_1 = 0 \tag{31}$$

$$q_2' + \zeta_4 q_2 + v_2 p_2 - \frac{\omega_1 \zeta_4}{\omega_2} q_1 = 0 \tag{32}$$

The eigen equation of the above system of equations is obtained from:

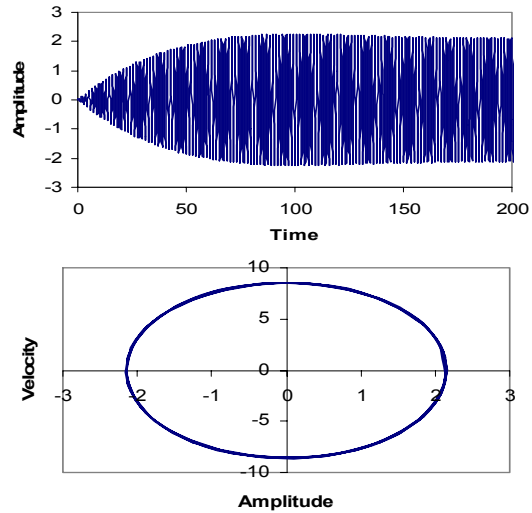


Fig. 2. Response of the tool holder without tool at primary resonance case  $\Omega \cong \omega_1, \zeta_1 = 0.02, \zeta_3 = 0.001, \eta_1 = 0.02, \eta_4 = 0.005, \Omega/\omega_1 = 1, F_1 = 0.5, F_2 = 0.25$ .

$$\begin{vmatrix} \lambda + (\zeta_1 + \zeta_2) & v_1 - \frac{\gamma_1}{2\omega_1} & \frac{\omega_2 \zeta_2}{\omega_1} & \frac{\gamma_1}{2\omega_1} \\ \left( v_1 - \frac{\gamma_1}{2\omega_1} + \frac{F_1}{2\omega_1 p_1} \right) & \lambda + (\zeta_1 + \zeta_2) & \frac{\gamma_1}{2\omega_1} & \frac{\omega_2 \zeta_2}{\omega_1} \\ \frac{\omega_1 \zeta_4}{\omega_2} & 0 & \lambda + \zeta_4 & -v_2 \\ 0 & \frac{\omega_1 \zeta_4}{\omega_2} & v_2 & \lambda + \zeta_4 \end{vmatrix} = 0 \tag{33}$$

The eigenvalues are given by the equation

$$\lambda^4 + r_1 \lambda^3 + r_2 \lambda^2 + r_3 \lambda + r_4 = 0 \tag{34}$$

where,  $r_1, r_2, r_3$  and  $r_4$  are functions of the parameters  $(a_1, a_2, \omega_1, \omega_2, \sigma_1, \sigma_2, F_1, \theta)$  and they are given in the appendix. According to the Routh-Hurwitz criterion, the necessary and sufficient conditions for all the roots of Eq. (34) to possess negative real parts is that

$$r_1 > 0, r_1 r_2 - r_3 > 0, r_3(r_1 r_2 - r_3) - r_1^2 r_4 > 0, r_4 > 0 \tag{35}$$

Investigation of the other two simultaneous resonance cases where  $\Omega \cong \omega_1/2, \omega_2 \cong \omega_1$  and  $\Omega \cong \omega_1/3, \omega_2 \cong \omega_1$  leads to similar Eqs. (24)-(27) with replacement of  $F_2$  and  $F_3$  instead of  $F_1$ ,

respectively. This means that all parameters have the same effect as the simultaneous primary case.

### 3. Results and discussion

The differential equation of the tool holder is solved numerically (applying Runge-Kutta 4th order method) at primary resonance case without tool as shown in Fig. 2. The steady state response is about

430% of (the fundamental) excitation amplitude  $F_1$ . The system is stable with fine limit cycle, denoting that the system is free from dynamic chaos.

#### 3.1 System behavior

Fig. 3(a), illustrates the results at simultaneous primary and internal resonance case when the tool is connected, i.e., when  $\Omega \cong \omega_1 \cong \omega_2$ . It can be seen for the tool holder that the steady state amplitude is 1.4%, but the steady state amplitude of the tool is about 62% of excitation amplitude  $F_1$ . This means that the effectiveness of the tool  $E_a$  ( $E_a = \text{the steady state amplitude of the tool holder without tool} / \text{the steady state amplitude of tool holder with tool}$ ) is about 307.

#### 3.2 Stability numerical results

The effects of different parameters were investigated by solving Eqs. (24)-(27). The results are illustrated graphically in Figs. 4 and 5. Both figures illustrate the occurrence of jump and saturation phenomena for two different cases of stability. Fig. 4(a) shows the effect of the detuning parameter  $\sigma_1$  on the steady state amplitude of the tool holder  $a_1$  for the stability of the case  $a_1 \neq 0, b_1 = 0$ .

Figs. 4(b), (c) show that the effects of increasing or decreasing the damping coefficients  $\zeta_1$  and  $\zeta_2$  on the steady state amplitude of the tool holder are trivial due to saturation occurrence. For increasing value of the non-linear parameter  $\gamma_1$ , the steady state amplitude of the tool holder is shifted and bent to the right, leading to the occurrence of the jump phenomena and multi-valued amplitudes as shown in Fig. 4(d). For negative and positive values of the non-linear parameters  $\eta_1$  and  $\eta_3$  the curve is bent to right or left leading to the occurrence of the jump phenomena and multi-valued amplitudes as shown in Figs. 4(e), (f).

For decreasing values of the natural frequencies  $\omega_1$  and  $\omega_2$  the steady state amplitude of the tool holder is bent to the right, leading to the occurrence of the jump phenomenon and multi-valued amplitudes as shown in Figs. 4(g), (h).

Fig. 4(i) shows that the steady state amplitude of the tool holder is a monotonic increasing function in its excitation amplitude  $F_1$ .

Fig. 5(a), shows the effect of the detuning parameter  $\sigma_2$  on the steady state amplitude of the tool  $b_1$  for the stability of the practical case  $a_1 \neq 0, b_1 \neq 0$ . In Fig. 5(b) the effect of increasing or decreasing the

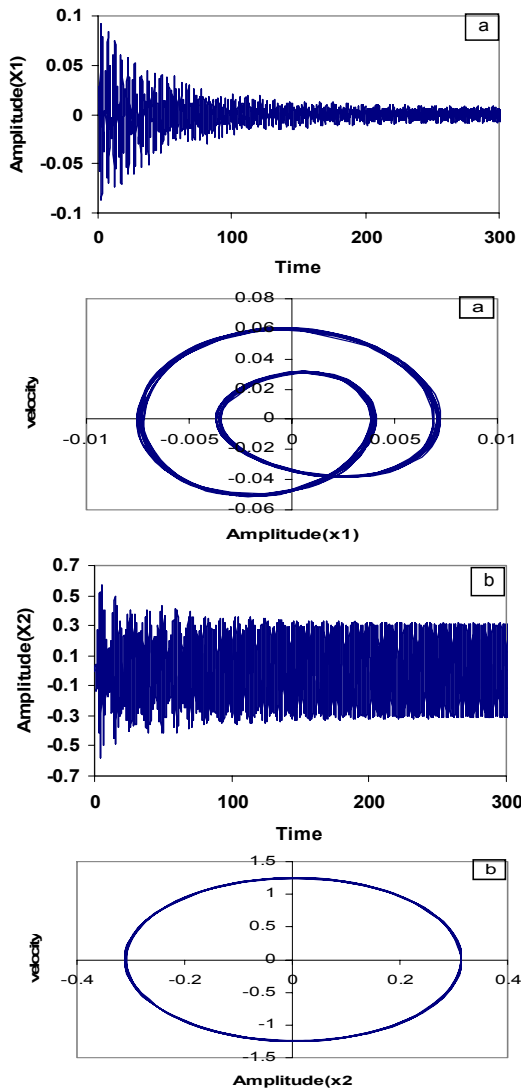


Fig. 3. Response of the tool holder and tool at simultaneous primary and internal resonance case  $\Omega \cong \omega_1 \cong \omega_2$  (a) the tool holder (b) the tool  $\zeta_1=0.02, \zeta_2=0.001, \zeta_3=0.001, \zeta_4=0.01, \gamma_1=1.6, \eta_1=0.02, \eta_2=0.02, \eta_3=0.005, \eta_4=0.005, \eta_5=0.2, \eta_6=0.05, \Omega/\omega_1=1, \omega_1=\omega_2$ .

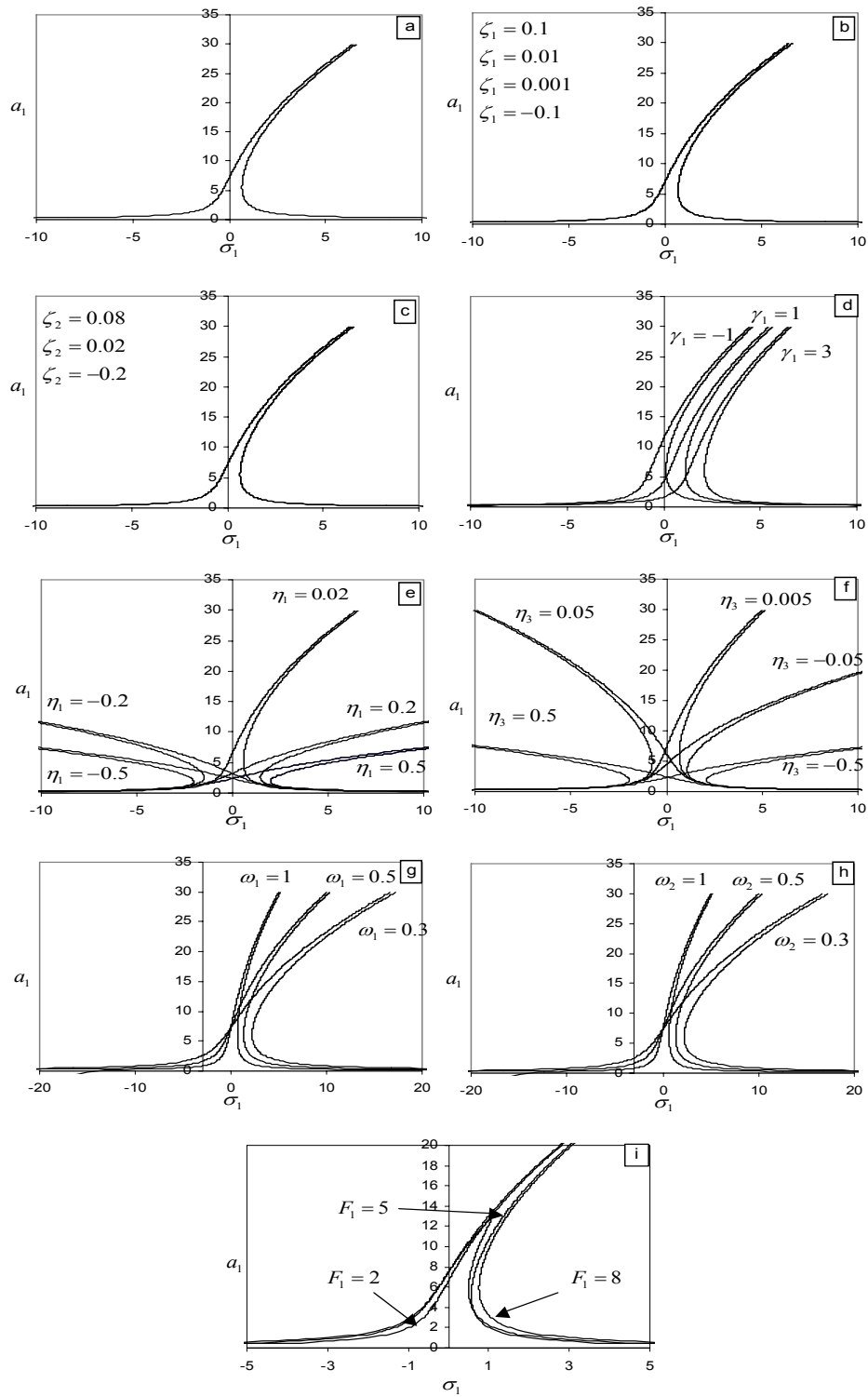


Fig. 4. Response curves (Different parameters against  $\sigma_1$ )  $\zeta_1 = 0.001, \zeta_2 = 0.02, \eta_1 = 0.02, \eta_3 = 0.005, \gamma_1 = 1, \omega_1 = 1, \omega_2 = 1, F_1 = 5$ .

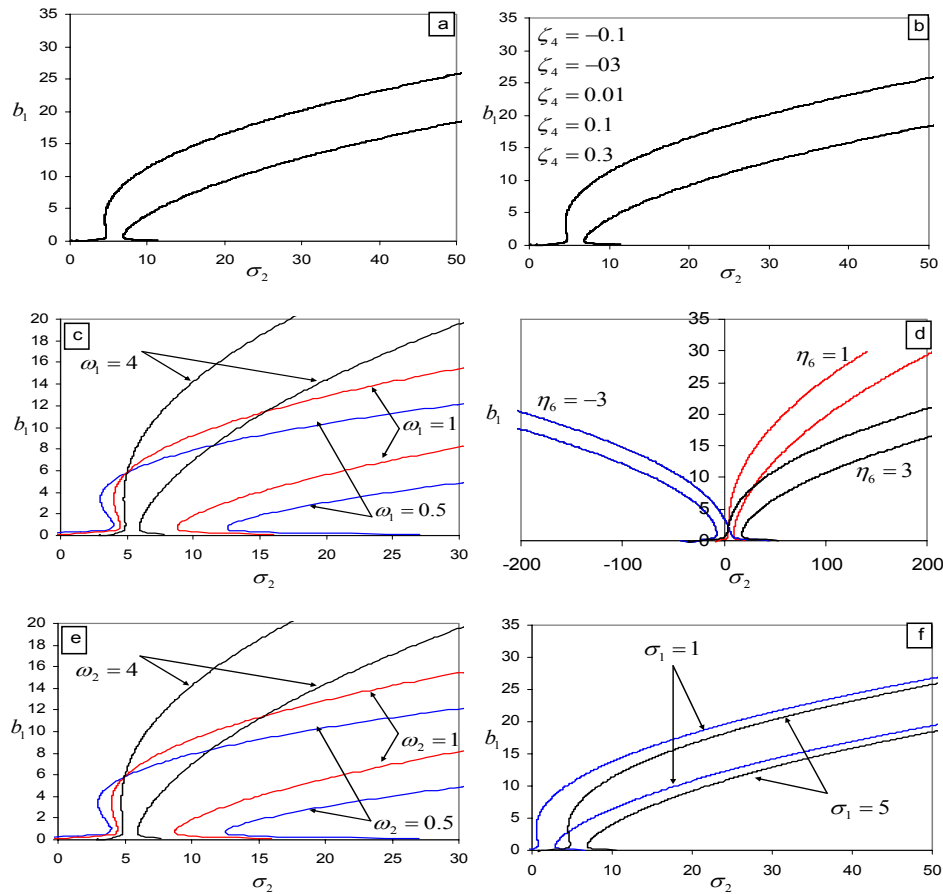


Fig. 5. Response curves (Different parameters against  $\sigma_2$ )  $\zeta_4=0.01$ ,  $\eta_6=3$ ,  $\omega_1=2$ ,  $\omega_2=2$ ,  $\sigma_1=5$ .

damping coefficient  $\zeta_4$  on the steady state amplitude of the tool is trivial due to saturation occurrence and the fact that the region of unstable solutions increases.

Figs. 5(c), (e) show that the steady state amplitude of the tool is a monotonic increasing function in the natural frequencies  $\omega_1$  and  $\omega_2$ , and the region of unstable solutions increases. For positive and negative value of the non-linear parameter,  $\eta_6$  the curve is bent to the right or left leading to the occurrence of the jump phenomenon and multi-valued amplitudes as shown in Fig. 5(d).

Fig. 5(f) shows that the steady state amplitude of the tool is a monotonic decreasing function in the detuning parameter  $\sigma_1$  and the region of unstable solutions increases.

### 3.3 Resonance cases

All extracted resonance cases were studied numerically. The results of worst cases are summarized in Table 2. It is clear that the best results have been obtained for the simultaneous primary and internal resonance case. This case gives the best results for tool holder vibration reduction and the reasonable high tool amplitude.

### 4. Conclusions

The vibrations of a second order, 2-DOF non-linear mechanical system (tool holder) and the tool were investigated. The physical motivation for the system stems from applications in ultrasonic machining in which an exciter drives a tuned blade having both linear and cubic non-linearities. The (USM) can be controlled by applying a non-linear tool. Multiple



Table 2. Summary of the worst resonance cases with and without tool.

Cases	Conditions	*Amplitude ratio ( $x_1/F_1$ ) without tool	Amplitude ratio ( $x_1/F_1$ ) with tool (tool holder)	Amplitude ratio ( $x_2/F_1$ ) (tool)	$E_a$	Remarks
$\Omega \cong \omega_1$	$\omega_2 \cong \omega_1$	430%	1.4 %	62 %	307	Limit cycle
	$\omega_2 \cong 2\omega_1$	430%	46 %	62 %	9.35	Limit cycle
	$\omega_2 \cong 3\omega_1$	430%	54 %	64 %	8	Limit cycle
	$\omega_2 \cong 4\omega_1$	430%	58%	62%	7.5	Limit cycle
$\Omega \cong 2\omega_1$	$\omega_2 \cong 2\omega_1$	8.6%	1.2 %	60%	7	Limit cycle
$\Omega \cong 3\omega_1$	$\omega_2 \cong 3\omega_1$	7.2%	1.18 %	60 %	6	Limit cycle
$\Omega \cong \frac{1}{2}\omega_1$	$\omega_2 \cong \frac{3}{2}\omega_1$	140%	5.4 %	8.6 %	26	Multi limit cycle
	$\omega_2 \cong \omega_1$	140%	1.8 %	9.5 %	78	Multi limit cycle
$\Omega \cong \frac{1}{3}\omega_1$	$\omega_2 \cong \omega_1$	50%	1.2 %	2.4 %	42	Multi limit cycle
	$\omega_2 \cong \frac{2}{3}\omega_1$	50%	2.8 %	8.4 %	18	Multi limit cycle

\* Amplitude ratio is the steady state amplitude divided by the excitation force amplitude. The multi limit cycles in Table 2 are shown in Fig. 6.

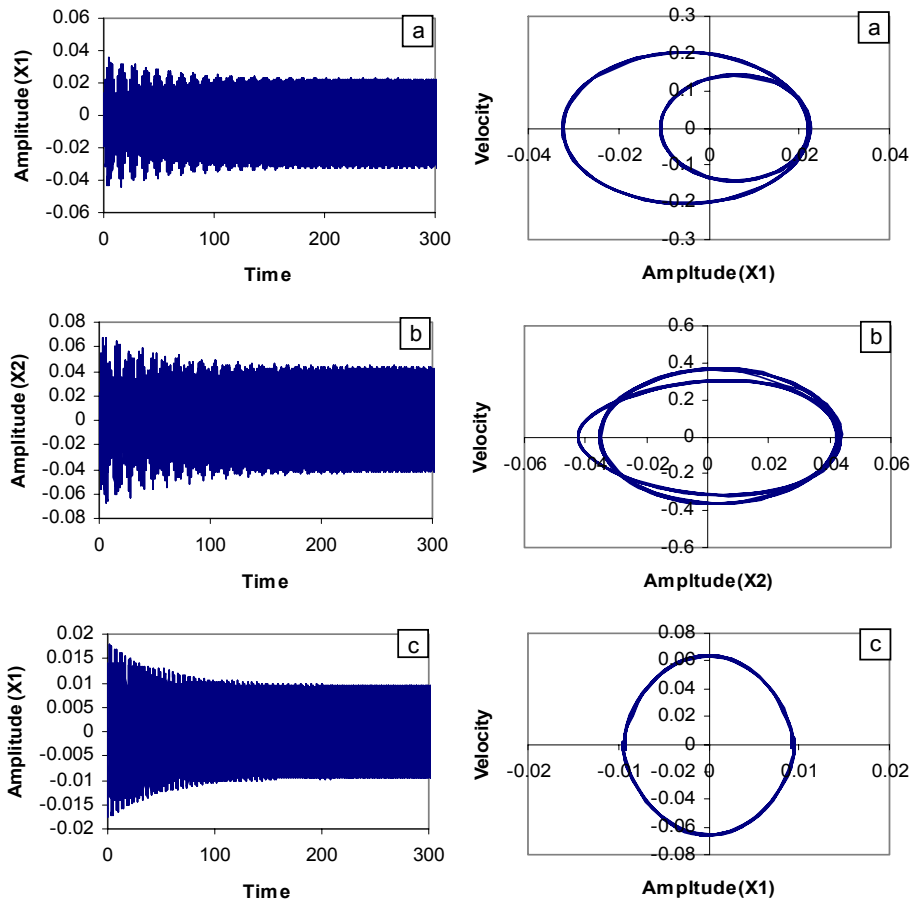


Fig. 6. (Continued)

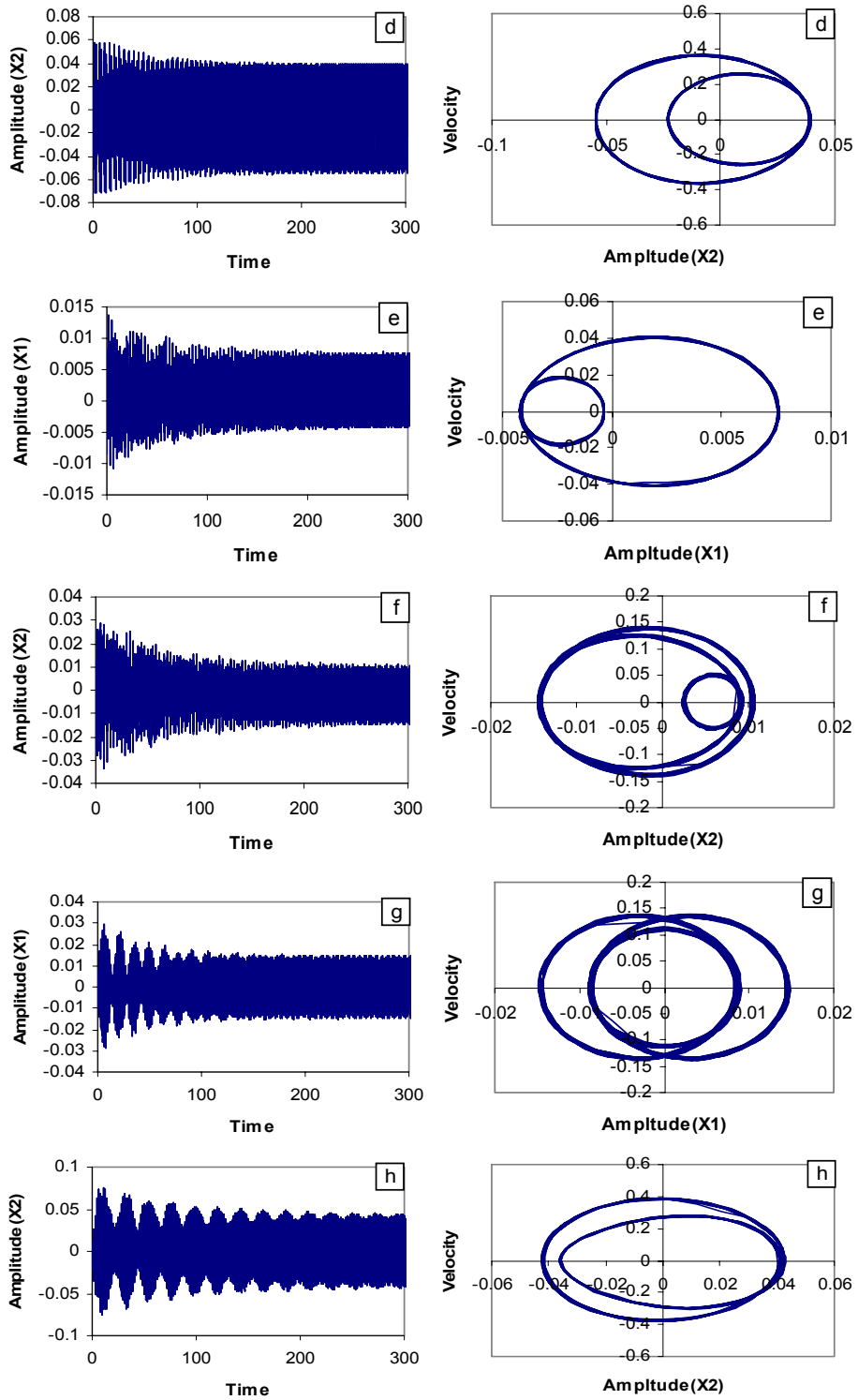


Fig. 6. The response of the cases  $\Omega \cong \omega_1/2, \omega_2 \cong 3\omega_1/2$ ,  $\Omega \cong \omega_1/2, \omega_2 \cong \omega_1$ ,  $\Omega \cong \omega_1/3, \omega_2 \cong \omega_1$ ,  $\Omega \cong \omega_1/3, \omega_2 \cong 2\omega_1/3$  respectively.

time scale perturbation technique was applied to determine semi-closed form solutions for the coupled differential equations up to the second order approximations. To study the stability of the system, the frequency response equations were applied and the phase-plane technique was used. From the above study the following may be concluded.

The proposed technique improves machine efficiency and saves machining time.

The worst behavior of the tool holder occurs at the primary resonance case where the steady state response is about 430% of the excitation amplitude  $F_1$ .

The vibration of the tool holder can be reduced via a tool and the effectiveness of the tool may be about  $E_a = 307$ , at simultaneous resonance case  $\Omega \cong \omega_1$ ,  $\omega_2 \cong \omega_1$ .

Optimum working conditions are obtained when  $\Omega \cong \omega_1$ ,  $\omega_2 \cong \omega_1$ , where the vibration of the tool holder is suppressed to about 1.4% of the original amplitude, and the tool has a reasonable amplitude about 62% of the fundamental amplitude  $F_1$ .

The reported results are in good agreement with Ref [21] regarding the amplitude reduction and saturation phenomenon occurrence. Also, the results confirmed the shift of the excitation frequency to the left at resonance, compared to the system natural frequency.

Next papers will deal with USM having multi-tools, to different excitation forces.

## Nomenclature

$c_j$ , (j=1,2,3)	: The damping coefficients of the tool holder and the tool .
$k_s$ , (s=1,2)	: The stiffness of the tool holder and the tool .
$h_n$ , (n=1,2,3,4)	: The non-linear parameters of the tool holder and the tool .
$F_j$ , $\Omega_j$ (j=1,2,3)	: The excitation amplitudes and frequencies.
$m_1, m_2$	: The masses of the tool holder and the tool.
$\zeta_s = c_s / 2m_s$ , (s=1,2)	: The linear damping coefficients of the tool holder.
$\zeta_3 = c_3 / m_1$	: The quadratic damping coefficient of the tool holder.

$\zeta_4 = c_2 / 2m_2$	: The damping coefficient of the tool.
$\eta_n = h_n / m_1$ , (n=1,2,3,4)	: The non-linear parameters of the tool holder.
$\eta_5 = h_2 / m_2$ , $\eta_6 = h_3 / m_2$	: The non-linear parameters of the tool.
$\omega_s^2 = k_s / m_s$ , (s=1,2)	: The natural frequencies of the tool holder and tool .
$\gamma_1 = k_1 / m_1$	: The stiffness of the tool holder.
$x_s$ , s=1,2	: Displacement of both tool holder and tool

## References

- [1] M.S. El Nachie, Stress, stability and chaos. *Mc Graw-Hill International Editions* (1992). Singapore. (1990) McGraw–Hill, United Kingdom.
- [2] A.H. Nayfeh and D.T. Mook, Nonlinear oscillations. New York: John Wiley (1979).
- [3] M.P. Cartmell and J. Lawson, Performance enhancement of an auto-parametric vibration absorber by means of computer control. *J. of Sound Vibration*. 177 (2) (1994) 173–195.
- [4] P. Woafa, H.B. Fotsin and J.C. Chedjou, Dynamics of two nonlinearity coupled oscillators. *Phys. Scripta*. 57 (1998) 195–200.
- [5] T.Y. Shen, Guo Weili and Y.C Pao, Torsional vibration control of a shaft through active constrained layer damping treatments. *J. of Vib. Acoust.* 119 (1997) 504–511.
- [6] K.R. Asfar, Effect of non-linearities in elastomeric material dampers on torsional vibration control. *Int. J. Non-linear. Mech* 27 (6) (1992)947–954.
- [7] M. Eissa and H.M. Abdelhafez, Stability and control of non-linear torsional vibrating systems. *Faculty of Engineering Alexandria University, Egypt* 41 (2) (2002) 343-353.
- [8] A.F. El-Bassiouny, Effect of non-linearities in elastomeric material dampers on torsional oscillation control. *J. Appl Math. Commun* 162 (2005) 835–854.
- [9] Cheng-Tang, Lee et al. Sub-harmonic vibration absorber for rotating machinery. *ASME J. Vib. Acoust* 119 (1997) 590–605.
- [10] M. Eissa, Vibration and chaos control in I.C engines subject to harmonic torque via non-linear ab-

sorbers. *ISMV-2000. In: Proc of Second International Symposium on Mechanical Vibrations. Islamabad, Pakistan, (2000).*

[11] M. Eissa and W El-Ganaini, Part I, Multi-absorbers for vibration control of non-linear structures to harmonic excitations. In: *Proc of ISMV Conference, Islamabad, Pakistan, (2000).*

[12] M. Eissa and W El-Ganaini, Part II, Multi-absorbers for vibration control of non-linear structures to harmonic excitations. In: *Proc of ISMV Conference, Islamabad, Pakistan, (2000).*

[13] M. Eissa, W El-Ganaini, and Y.S. Hamed, Saturation, stability and resonance of nonlinear systems. *Physica A* 356 (2005) 341-358.

[14] M. Eissa, W El-Ganaini, and Y.S. Hamed, Optimum working conditions of a non-linear SDOF system to harmonic and multi-parametric excitations. *Scientific Bulletin, Part III : Mechanical Engineering and Physics & Mathematics faculty of engineering, Ain Shams university* 40 (1) (2005) 1113-1127.

[15] M. Eissa, W El-Ganaini, and Y.S. Hamed, On the saturation Phenomena and resonance of non-linear differential equations. *Minufiya Journal of Electronic Engineering Research MJEER* 15 (1) (2005) 73-84.

[16] M. Eissa and M. Sayed, A Comparison between active and passive vibration control of non-linear simple pendulum, Part I: Transversally tuned absorber and negative  $G\dot{\varphi}^n$  feedback. *Math and Comput Appl* 11 (2) (2006) 137-149.

[17] M. Eissa and M. Sayed, Comparison between active and passive vibration control of non-linear simple pendulum, Part II: Longitudinal tuned absorber  $G\ddot{\varphi}^n$  and negative  $G\dot{\varphi}^n$  feedback. *Math and Comput Appl* 11 (2) (2006) 151-162.

[18] M. Eissa, S. EL-Serafi, H. El-Sherbiny and T.H. El-Ghareeb, Comparison between passive and active control of non-linear dynamical system. *Japan J of Ind and Appl Math* 23 (2) (2006) 139-161.

[19] M. Eissa, S. EL-Serafi, H. El-Sherbiny and T.H. El-Ghareeb, On passive and active control of vibrating system. *Int. J. of Appl. Math* 18 (4) (2005) 515-537.

[20] M. Eissa, S. EL-Serafi, H. El-Sherbiny and T.H. El-Ghareeb, 1:4 Internal resonance active absorber for non-linear vibrating system, *Int. J. of pure and Appl. Math* 28 (1) (2006) 515-537.

[21] F.C. Lim, M.P. Cartmell, A. Cardoni and M. Lucas, A preliminary investigation into optimizing

the response of vibrating systems used for ultrasonic cutting. *J. Sound. Vib* 272 (2004) 1047–1069.

[22] Y.A. Amer, Vibration control of ultrasonic cutting via dynamic absorber. *Chaos, Solitons & Fractals* 34 (2) (2007) 1328-1345.

**Appendix**

$$k_1 = \frac{3(\eta_3 - \eta_1)a_1^2}{4\omega_1} - \frac{\gamma_1}{\omega_1}$$

$$k_2 = \frac{\gamma_1^2}{4\omega_1^2} + \frac{9(\eta_3 - \eta_1)^2 a_1^4}{64\omega_1^2} - \frac{3\gamma_1(\eta_3 - \eta_1)a_1^2}{8\omega_1^2}$$

$$+ \frac{(\omega_1\zeta_1 + \omega_1\zeta_2)^2}{\omega_1^2} - \frac{F_1^2}{4\omega_1^2 a_1^2}, \quad k_3 = -\frac{3\eta_6 b_1^2}{4\omega_2} - 2\sigma_1$$

$$k_4 = \sigma_1^2 + \frac{9\eta_6^2 b_1^4}{64\omega_2^2} + \frac{3\eta_6 b_1^2 \sigma_1}{4\omega_2} + \zeta_4^2$$

$$k_5 = \frac{3(\eta_3 - \eta_1)a_1^2}{4\omega_1} - \frac{\gamma_1}{\omega_1} + \frac{3\eta_3 b_1^2}{2\omega_1} \quad R_1 = \frac{\gamma_1 b_1}{2} - \frac{3\eta_3 b_1^3}{8}$$

$$k_6 = \frac{\gamma_1^2}{4\omega_1^2} + \frac{9(\eta_3 - \eta_1)^2 a_1^4}{64\omega_1^2} + \frac{27\eta_3^2 b_1^4}{46\omega_1^2} - \frac{3\gamma_1(\eta_3 - \eta_1)a_1^2}{8\omega_1^2}$$

$$- \frac{3\gamma_1\eta_3 b_1^2}{4\omega_1^2} + \frac{9\eta_3(\eta_3 - \eta_1)a_1^2 b_1^2}{16\omega_1^2} + \frac{(\omega_1\zeta_1 + \omega_1\zeta_2)^2}{\omega_1^2}$$

$$- R_1^2 - \frac{\omega_2^2 \zeta_2^2 b_1^2}{\omega_1^2 a_1^2} - \frac{F_1^2}{4\omega_1^2 a_1^2} - R_1 F_1 - \frac{3R_1\eta_3 b_1^2}{4\omega_1^2 a_1} - \frac{3F_1\eta_3 b_1^2}{8\omega_1^2 a_1}$$

$$- \frac{81\eta_3^2 a_1^2 b_1^2}{64\omega_1^2} + \frac{9R_1\eta_3 b_1}{4\omega_1^2} + \frac{9\eta_3 b_1 F_1}{8\omega_1^2} + \frac{27\eta_3^2 a_1 b_1^3}{32\omega_1^2}$$

$$k_7 = \frac{3\eta_6 a_1^2}{2\omega_2} + \frac{3\eta_6 b_1^2}{4\omega_2} + 2\sigma_1$$

$$k_8 = \sigma_1^2 + \frac{3\eta_6 a_1^2 \sigma_1}{2\omega_2} + \frac{3\eta_6 b_1^2 \sigma_1}{4\omega_2} + \frac{27\eta_6^2 a_1^4}{64\omega_2^2} + \frac{9\eta_6^2 b_1^4}{64\omega_2^2}$$

$$+ \zeta_4^2 - \frac{45\eta_6 a_1^2 b_1^2}{64\omega_2^2} - \frac{9\eta_6^2 a_1^6}{64\omega_2^2 b_1^2} - \frac{\omega_1^2 \zeta_4^2 a_1^2}{\omega_2^2 b_1^2} + \frac{9\eta_6^2 a_1^5}{32\omega_2^2 b_1}$$

$$- \frac{27\eta_6^2 a_1^4}{32\omega_2^2} + \frac{27\eta_6^2 a_1^3 b_1}{32\omega_2^2}, \quad r_1 = 2\zeta_4 + 2\zeta_1 + 2\zeta_2$$

$$r_2 = \zeta_1^2 + \zeta_2^2 + 4\zeta_1\zeta_4 + \zeta_4^2 + v_1^2 + 2\zeta_2\zeta_4 + 2\zeta_1\zeta_2 + v_2^2$$

$$- \omega_1 v_1 \gamma_1 + \frac{\omega_1^2 \gamma_1^2}{4} + \frac{v_1 F_1}{2\omega_1 P_1} - \frac{\gamma_1 F_1}{4P_1}$$

$$r_3 = 2\zeta_1\zeta_4 - \frac{\omega_1 \zeta_4 \gamma_1^2}{2\omega_2} - 2\omega_1 v_1 \gamma_1 \zeta_4 + 2\zeta_1 v_2^2 + 2\zeta_1^2 \zeta_4$$

$$- \frac{\zeta_4 \gamma_1 v_2}{\omega_2} + \frac{\omega_1^2 \gamma_1^2 \zeta_4}{2} + \frac{v_1 \gamma_1 \zeta_4}{\omega_2} + 2\zeta_2 v_2^2 + 2\zeta_1 \zeta_4^2$$

$$+ 2v_1^2 \zeta_4 - \frac{F_1 \zeta_4 \gamma_1}{2P_1} + \frac{F_1 \zeta_4 v_1}{\omega_1 P_1} + \frac{F_1 \zeta_4 \gamma_1}{4\omega_1 \omega_2 P_1}$$

$$\begin{aligned}
r_4 = & 2\zeta_1\zeta_2v_2^2 + \frac{\omega_1^2\gamma_1^2\zeta_4^2}{4} + \frac{\omega_1^2\gamma_1^2v_2^2}{4} + \zeta_1^2v_2^2 + v_1^2v_2^2 \\
& + \frac{\zeta_4^2\gamma_1^2}{4\omega_2^2} - \frac{\omega_1\zeta_4^2\gamma_1^2}{2\omega_2} + v_1^2\zeta_4^2 + \zeta_2^2v_2^2 - \frac{\zeta_2\zeta_4\gamma_1v_2}{\omega_2} - \frac{\zeta_1\zeta_4\gamma_1v_2}{\omega_2} \\
& - 2v_1\zeta_4\zeta_2\gamma_1v_2 + \frac{v_1\zeta_4^2\gamma_1}{\omega_2} - \omega_1v_1\gamma_1\zeta_4^2 - \frac{F_1v_2^2\gamma_1}{4P_1} - \frac{F_1\zeta_4\zeta_2v_2}{2\omega_1P_1} \\
& + \zeta_1^2\zeta_4^2 - \omega_1v_1\gamma_1v_2^2 + \omega_1\gamma_1\zeta_4\zeta_2v_2 + \frac{F_1\zeta_4^2v_1}{2\omega_1P_1} \\
& + \frac{F_1v_2^2v_1}{2\omega_1P_1} + \frac{F_1\zeta_4^2\gamma_1}{4\omega_1\omega_2P_1} - \frac{F_1\zeta_4^2\gamma_1}{4P_1} \\
& + \zeta_1^2\zeta_4^2 - \omega_1v_1\gamma_1v_2^2 + \omega_1\gamma_1\zeta_4\zeta_2v_2 + \frac{F_1\zeta_4^2v_1}{2\omega_1P_1}
\end{aligned}$$



**M. M. Kamel** received his B.S. degree in Mathematics from Ain Shams University, EGYPT, in 1979. He then received his M.S.c degrees from Ain Shams University, in 1986 and Ph.D. degrees from Menofia University, in 1994. Dr. M. M.

Kamel is currently an Associate Professor of Mathematics at the Department of Engineering Mathematics, Faculty of Electronic Engineering Menofia University, Egypt. Dr. M. M. Kamel research interests include Differential equations, Numerical Analysis, and Vibration control.



**W. A. A. El-Ganini** received her B.S. degree in Mathematics from Ain Shams University, EGYPT, in 1980. She then received her M.S.c and Ph.D. degrees from Suez Canal University, in 1984 and 1989, respectively. Dr. W. A. A. El-Ganini is currently an

Assistant Professor of Mathematics at the Department of Engineering Mathematics, Faculty of Electronic Engineering Menofia University, Egypt. Dr. W. A. A. El-Ganini research interests include Differential equations, Numerical Analysis, and Vibration control.



**Y. S. Hamed** received his B.S. degree in Mathematics from Menofia University, EGYPT, in 1998. He then received his M.S.c and Ph.D. degrees from Menofia University, in 2005 and 2009, respectively. Dr. Y. S. Hamed is currently an Assistant

Professor of Pure Mathematics at the Department of Engineering Mathematics, Faculty of Electronic Engineering Menofia University, Egypt. Dr. Y. S. Hamed research interests include Differential equations, Numerical Analysis, and Vibration control.